ORIGINAL ARTICLE

Human and mouse neuroinflammation markers in Niemann-Pick disease, type C1

**Stephanie M. Cologna · Celine V. M. Cluzeau ·
Nicole M. Yanjanin · Paul S. Blank · Michelle K. Dail ·
Stephan Siebel · Cynthia L. Toth · Christopher A. Wassif ·
Andrew P. Lieberman · Forbes D. Porter**

Abstract Niemann-Pick disease, type C1 (NPC1) is an autosomal recessive lipid storage disorder in which a pathological cascade, including neuroinflammation occurs. While data demonstrating neuroinflammation is prevalent in mouse models, data from NPC1 patients is lacking. The current study focuses on identifying potential markers of neuroinflammation in NPC1 from both the *Npc1* mouse model and NPC1 patients. We identified in the mouse model significant changes in expression of genes associated with inflammation and compared these results to the pattern of expression in human cortex and cerebellar tissue. From gene expression array analysis, complement 3 (*C3*) was increased in mouse and human post-mortem NPC1 brain tissues. We also characterized protein levels of inflammatory markers in cerebrospinal fluid (CSF) from NPC1 patients and controls. We found increased levels of interleukin 3, chemokine (C-X-C motif) ligand 5, interleukin 16 and chemokine ligand 3 (CCL3), and decreased levels of interleukin 4, 10, 13 and 12p40 in CSF from NPC1 patients. CSF markers were evaluated with respect to phenotypic severity. Miglustat treatment in NPC1 patients slightly decreased IL-3, IL-10 and IL-13 CSF levels; however, further studies are needed to establish a strong effect of miglustat on inflammation markers. The identification of inflammatory markers with altered levels in the cerebrospinal fluid of NPC1 patients may provide a means to follow secondary events in NPC1 disease during therapeutic trials.

S. M. Cologna · C. V. M. Cluzeau · N. M. Yanjanin · M. K. Dail ·
S. Siebel · C. L. Toth · C. A. Wassif · F. D. Porter (✉)
Program in Developmental Endocrinology and Genetics, Section on Molecular Dysmorphology, NICHD, NIH, DHHS, Bld. 10, Rm. 9D42, 10 Center Dr,
Bethesda, MD 20892, USA
e-mail: fdporter@mail.nih.gov

P. S. Blank
Program in Physical Biology, Section on Membrane & Cellular Biophysics, NICHD, NIH, DHHS, Bethesda, MD 20892, USA

A. P. Lieberman
Department of Pathology, University of Michigan, Ann Arbor, MI 48109, USA

Introduction

Niemann-Pick disease, type C1 (NPC1) is a fatal, genetic disorder that results in severe, progressive neurodegeneration. Mutations of the *NPC1* gene result in a loss of function of the NPC1 protein (Carstea et al 1997), thereby, impairing cholesterol and glycosphingolipid trafficking. A deficiency of NPC1 protein function results in an accumulation of unesterified cholesterol and glycosphingolipids in the late endosomes/lysosomes (Pentchev et al 1987; Zervas et al 2001; Vanier and Millat 2003). Following the initial defect, a complex cascade of pathological events occurs in NPC1 including oxidative stress (Reddy et al 2006; Zampieri et al 2009; Fu et al 2010; Porter et al 2010; Klein et al 2011; Vazquez et al 2011), neurofibrillary tangle formation (Love

et al 1995; Suzuki et al 1995), and neuronal apoptosis among others (Ong et al 2001; Sarna et al 2003; Wu et al 2005). Clinical symptoms in NPC1 patients are heterogeneous and include hepatosplenomegaly, ataxia, vertical gaze palsy, and dementia, in which progression in neurological severity occurs over time (Vanier 2010; Yanjanin et al 2010). To date, there is no FDA-approved therapy for NPC1. However, reports have indicated that treatment with miglustat, (Zavesca®), an imino sugar that blocks glycosphingolipid synthesis, slows the neurological progression of the disease in both animal models and NPC1 patients (Patterson et al 2007; Pineda et al 2009; Patterson et al 2010; Wraith et al 2010). Miglustat has been approved for the treatment of NPC1 by the European Medicines Agency. Currently, miglustat is only FDA-labeled for the treatment of Gaucher disease but has been used off-label for NPC1. Recently, 2-hydroxypropyl-β-cyclodextrin (HP-β-CD) has shown promise as a potential therapy for NPC1. HP-β-CD has been demonstrated to maintain neurological function and reduce the storage burden in both mouse and feline models of NPC1 disease (Davidson et al 2009; Liu et al 2009; Ramirez et al 2010; Ward et al 2010; Aqul et al 2011).

Neuroinflammation is a common feature found in many disorders particularly those affecting the central nervous system (CNS). Within the CNS, the innate immune system of microglia, astrocytes and perivascular macrophages serve as a first line of defense (Graeber et al 2011; Veerhuis et al 2011). The activation of microglia and astrocytes during the inflammation process results in a morphological change and is characterized by positive staining for CD68 and GFAP, respectively (Eng et al 2000; Kunisch et al 2004; Marin-Teva et al 2012). Secreted proteins from both microglia and astrocytes can be used as inflammation markers in cerebrospinal fluid-based analyses [as reviewed (Suk 2010)].

The first evidence of neuroinflammation in the *Npc1* mouse is the activation of microglia at approximately 2 weeks post birth. This activation begins the neurodegenerative cascade with subsequent marked activation of astrocytes around 4 weeks post birth, beneath the Purkinje cell layer corresponding to the sites of early apoptosis in NPC1 disease (Baudry et al 2003). Smith et al tested the effectiveness of non-steroidal anti-inflammatory drugs in *Npc1* mutant mice where a positive response with respect to survival was observed, as well as reduced microglial activation (Smith et al 2009). Pressey and co-workers investigated the effect of *Npc1* deficiency on brain pathology at different stages of the disease process (Pressey et al 2012). The thalamus and cerebellum have been identified as particularly vulnerable to neurodegeneration, showing early activation of glia from 3 weeks post birth (Pressey et al 2012). The relationship between glia and neurons is variable within different brain regions, suggesting that the mechanism underlying the neuroinflammation in various brain regions

may differ. Recently miglustat treatment in the feline model of NPC1 was shown to improve Purkinje cell survival, and reduced lipid storage and microglial activation suggesting that neuroinflammation may be affected with miglustat (Stein et al 2012).

Microglial activation in chronic neurodegeneration can be beneficial, harmful or non-significant (Ransohoff and Brown 2012). The role of inflammation in the disease progression of NPC1 has yet to be determined. It is particularly unclear whether neuroinflammation is a primary pathological process, or a secondary event resulting from the initial genetic and trafficking defects. Recent data suggest that neuroinflammation in NPC1 is a secondary process (Lopez et al 2012a, b). While some studies have discussed the prevalence of inflammation in *Npc1* mouse brain tissue and the potential benefit of anti-inflammatory treatment, human studies are lacking. Understanding the role of neuroinflammation and identification of biomarkers associated with this aspect of NPC1 pathology will be of utility in designing and translating potential therapies to NPC1 patients.

In an effort to further characterize and potentially target therapeutic interventions along the neuropathogenic cascade in NPC1, we sought to further understand the neuroinflammation processes occurring in both *Npc1* mice and NPC1 patient brain tissue using differential expression analysis. Our work additionally aimed at establishing which inflammatory markers are altered in the cerebrospinal fluid from NPC1 patients relative to controls. Using discovery and targeted based approaches, several inflammation markers were found to be altered in the *Npc1* mouse model as well as in cerebrospinal fluid from NPC1 patients. These data will provide a more comprehensive understanding of the array of biological processes that are involved in NPC1 pathology and provide a deeper understanding of the disease process while concurrently providing potential biomarkers for monitoring disease progression and evaluating potential therapeutic agents' efficacy.

Materials and methods

Animal breeding and tissue isolation Animal work was performed under an NICHD Animal Care and Use Committee-approved animal study protocol. Heterozygous $Npc1^{+/-}$ mice (BALB/c Nctr-$Npc1^{m1N}$/J strain) were intercrossed to obtain control ($Npc1^{+/+}$) and mutant ($Npc1^{-/-}$) littermates. For tissue collection, female $Npc1^{-/-}$ and $Npc1^{+/+}$ mice were sacrificed at 1, 3, 5, 7, 9 and 11 weeks of age using a rising concentration of carbon dioxide. The cerebral cortex was collected, flash frozen and stored at −80 °C until use. Mice homozygous for the *Ccl3*-targeted mutation (B6.129P2-$Ccl3^{tm1Unc}$/J strain,

C57BL/6 genetic background) were used to test the effect of *Ccl3* deficiency on the NPC1 pathological process. Pups were weaned 3 weeks after birth and subsequently had free access to water and standard mouse chow. PCR genotyping was performed using tail DNA. Primers and PCR conditions to genotype the *Npc1* locus were previously described (Loftus et al 1997). *Ccl3* locus genotype was determined using two pairs of primers: the wild-type allele was amplified using the sense $^{5'}$ATGAAGGTCTCCACCACTGC$^{3'}$ and the antisense $^{5'}$AGTCAACGATGAATTGGCG$^{3'}$ (yielding a 668 bp fragment); the mutant allele was amplified using the sense $^{5'}$CTTGGGTGGAGAGGCTATTC$^{3'}$ and the antisense $^{5'}$AGGTGAGATGACAGGAGATC $^{3'}$ (yielding a 280 bp fragment). The PCR conditions were as follows: 94 °C x 3 min., then 35 cycles of: 94 °C×30 s., 66 °C×1 min., and 72 °C×1 min. The final step was to heat at 72 °C×7 min and hold at 4 °C until further analysis. *Ccl3*$^{-/-}$ mice were intercrossed with *Npc1*$^{+/-}$ mice to generate double-heterozygous animals, which were then backcrossed to *Npc1*$^{+/-}$ for five generations. Double heterozygous animals from the N5 generation were then intercrossed to generate *Npc1*$^{+/+}$*Ccl3*$^{+/+}$, *Npc1*$^{-/-}$*Ccl3*$^{+/+}$, *Npc1*$^{-/-}$*Ccl3*$^{+/-}$ and *Npc1*$^{-/-}$*Ccl3*$^{-/-}$ animals. Weight measurements were determined twice a week from 4 weeks of age. Animals were euthanized according to the ACUC protocol when they had lost 20 % of their maximal weight, and this was defined as the age of death for survival analysis.

Human studies Human post-mortem tissue from age-matched control and NPC1 patients was obtained from the NICHD Blood and Tissue Bank (http://medschool.umaryland.edu/btbank/). Cerebellar tissue was obtained from controls UMB#754 (asthma attack), UMB#914 (motor vehicle accident), UMB#1841 (motor vehicle accident), UMB#5282 (asphyxia) and from NPC1 patients (confirmed mutations annotated from NM_000271.4) UMB#4237 (c.1628C>T/not detected), UMB#4770 (c.3107C>T/c.3573_3574insACTT), UMB#5372 (c.2842G>A/c.3182 T>C), UMB#M4002M (c.973_974dup/not detected). Frontal cortex tissue was received from NPC1 patients UMB#4237, UMB#4770, UMB#5372, UMB#M4002M, UMB#4214 (apparent c.3182 T>C homozygosity), UMB#M4003M (c.3134_3135insG/c.3566A>G), UMB#M4004M (c.2819C>T/c.3182 T>C) and controls UMB#754, UMB#914, UMB#1841, UMB#5282, UMB#1573 (motor vehicle accident), UMB#4670 (accident), UMB#5387 (drowned). No other data are available on these individuals.

NPC1 patients included in this study were enrolled between August 2006 and January 2011 in an Institutional Review Board-approved, longitudinal, Natural History/Observational trial at the National Institutes of Health (06-CH-0186, NCT00344331). Written, informed consent was obtained for all subjects. Assent was obtained when appropriate. Clinical diagnosis was confirmed by filipin staining of fibroblasts and *NPC1* mutation analysis. Cerebrospinal fluid was collected via lumbar puncture. Control cerebrospinal fluid was obtained from 30 gender and age-matched patients who were undergoing cerebrospinal collection for another clinical indication. Four control patients were febrile (>38.5 °C) at the time of cerebrospinal fluid collection, but none had elevated white blood cell count or positive cultures. Age of control subjects ranged from 2 weeks to 20 years at the time of cerebrospinal fluid collection.

Cerebrospinal fluid biomarker measurements were made by Rules Based Medicine (Austin, TX) utilizing Multi-Analyte Profiling Technology. Statistical calculations were performed using GraphPad Prism. Log$_{10}$ transformed concentration values were used to perform statistical analyses on normally distributed datasets. The D'Agostino and Pearson omnibus normality test was used. For cases in which less than 40 % of the total number of measurements was missing due to being below the limit of detection (LOD), the LOD/2 substitution method was used (Ganser and Hewett 2010). C3 concentrations in CSF of a subset of NPC1 patients covering the full age and severity range and controls (*N*=14 and 11 respectively) were measured using the GenWay Biotech kit, according to the manufacturer's recommendations. A 1:20 dilution of the CSF samples was used to bring the sample concentration into the assay concentration range.

RNA isolation Frozen tissue samples, from a single mouse cortex, or approximately 100 mg from post-mortem human tissue, were homogenized in TRIzol (Life Technologies, Carlsbad, California) using Omni-Tips^{TM} (Omni International, Marietta, GA). After chloroform addition and phase separation, total RNA was purified using the RNeasy Mini Kit (Qiagen, Valencia, CA) with an on-column DNase digestion step using the RNase-Free DNase Set (Qiagen, Valencia, CA).

PCR arrays Following RNA extraction, total 7-week-old mouse or human RNA (1 μg) was reverse-transcribed using the RT^2 First strand kit (SA Bioscience), as recommended by the manufacturer. The Mouse Inflammatory Cytokines and Receptors PCR Array (SA Bioscience) was performed using cerebral cortex tissue cDNA (*N*=3) according to the manufacturer's protocol. The Human Inflammatory Cytokines and Receptors PCR Array (SA Bioscience) was performed on both the human frontal cortex and cerebellum according to the manufacturer's protocol (*N*=3; NPC1 patients UMB#4237, 5372, M4002M, and controls UMB#754, 914, 1841). Genes for which an undetermined Ct value was reported in at least one sample were excluded from analysis. All raw data are available in Supplemental Table 1.

Validation of PCR array data Total RNA (10 μg) was reverse-transcribed into cDNA according to the manufacturer's

Table 1 Genes significantly altered in cerebral cortex tissue from 7-week $Npc1^{-/-}$ mice relative to control ($Npc1^{+/+}$) mouse tissue. A total of 12 transcripts were altered with a fold-change of ≥2 ($p \leq 0.1$)

Gene symbol	p-value	Fold-change
C3	0.04	3.8
Ccl11	0.09	2.7
Ccl3	0.01	6.3
Ccl4	0.06	3.5
Ccl5	0.03	2.1
Ccl8	0.03	7.6
Cxcl1	0.02	4.1
Cxcl10	0.01	7.7
Cxcl11	0.03	2.9
Il1a	0.07	2.2
Il1b	0.04	3.6
Il1r2	0.06	2.0

instructions using the High-Capacity cDNA archive kit (Applied Biosystems). The following TaqMan assays (Applied Biosystems) were used to assess the expression level of several genes with altered expression including: *Ccl8* (Mm01297183), *Il1b* (Mm01336189), *Cxcl9* (Mm00434946), *C3* (Mm00437858) and *Cxcl10* (Mm00445235); *C3* (Hs01100879), *C4A* (Hs00167147), *CXCL3* (Hs00171061), *CXCL5* (Hs01099660), *IL10RA* (Hs00155485), *CEBP* (Hs00270923), *TOLLIP* (Hs01553188) *SPP1* (Hs00959010), *CCR5* (Hs00152917), and *CCL5* (Hs00174575). All gene assays were first validated using serial dilutions of control cDNA and compared to *Gapdh/GAPDH* (mouse *Ccl8*, *Cxcl9*, *Il1b*, and *Cxcl10* assays; human *CXCL3*, *CXCL5*, *CEBP*, *CCR5*, *TOLLIP*, and *SPP1* assays), or *Actb/ACTB* assays (mouse *C3* assay; human *C3*, *C4A*, *CCL5* and *IL10RA* assays). We were unable to confirm the probes for the following genes due to low expression levels in the tissues we tested: *LTB*, *IL1F9*, *IL5* and *IL9R*.

Quantitative real-time PCR (qPCR) was performed using an Applied Biosystems 7900 real-time PCR system. Each sample was analyzed in triplicate, using 50 ng of total cDNA for each reaction. Human gene expression was validated on the full set of NPC1 patients and controls available (seven samples for each group for frontal cortex; four samples for each group for cerebellum). Mouse gene expression was validated on the 7-week-old samples used for the PCR array, as well as on an independent set of 1, 3, 5, 7, 9, and 11 week-old samples. The relative quantification of gene expression was performed with the comparative cycle number measured with the threshold method (C_T) (Livak and Schmittgen 2001), using the control samples as a reference for quantification, and was plotted with mean and standard deviation (SD). Log_{10} transformed quantitation values were used to

perform statistical analyses on normally distributed datasets. An unpaired *t*-test with Welch's correction, when appropriate, was performed to assess the significance of the difference of means between control and mutant or patient samples. A list of all genes or proteins analyzed in this study is provided in Supplemental Table 1.

Pathology study on human brain post-mortem sample Fixed tissue slices embedded in paraffin were obtained from the NICHD Brain and Tissue Bank for three patients and controls. Tissues were stained using a mouse anti-Human CD68 antibody (EBM11, Dako) and developed using the Vectastain ABC kit (Vector) using standard protocols.

Results

Expression of genes associated with inflammation in *Npc1* mutant mouse cerebral cortex tissue

7-Week Npc1 mouse analysis We conducted an inflammation-targeted gene expression analysis from cerebral cortex tissue isolated from 7-week-old $Npc1^{+/+}$ and $Npc1^{-/-}$ mice. Twelve genes (Table 1) met our screening criteria of an absolute fold-change ≥2 and p-value ≤0.1. These 12 genes include members of the complement pathway, cytokine/chemokine family and the interleukin family. *Il1b*, *Ccl8*, *C3*, *Cxcl9* and *Cxcl10* genes were further validated via qPCR (Supplemental Fig. 1) with significantly increased expression of *Il1b*, *Ccl8* and *Cxcl10* genes. *C3* and *Cxcl9* expression appeared to be increased; however, not significantly (p-values 0.06 and 0.17 respectively), likely due to the high variability in expression levels for *C3* and *Cxcl9* in the mutant and control groups respectively.

Npc1 mouse model inflammation time course study We additionally investigated the mRNA expression of the same five genes listed above as well as *Ccl3* in an independent set of *Npc1* mouse cerebral cortex tissue collected at 1, 3, 5, 7, 9 and 11 weeks of age (Fig. 1). The expression of all genes analyzed with the exception of *Ccl8* was significantly increased in the $Npc1^{-/-}$ mouse tissue compared to control littermates from 3 weeks of age across the time course study. Only *Cxcl10* expression was found to be significantly increased at the 1 week time point.

Effect of Ccl3 up-regulation in Npc1 pathological process

Ccl3 gene expression has previously been described as increased in the *Npc1* mouse model (Liu et al 2010; Aqul et al 2011; Lopez et al 2012a). Our time course study indicated an early alteration of *Ccl3* expression (Fig. 1),
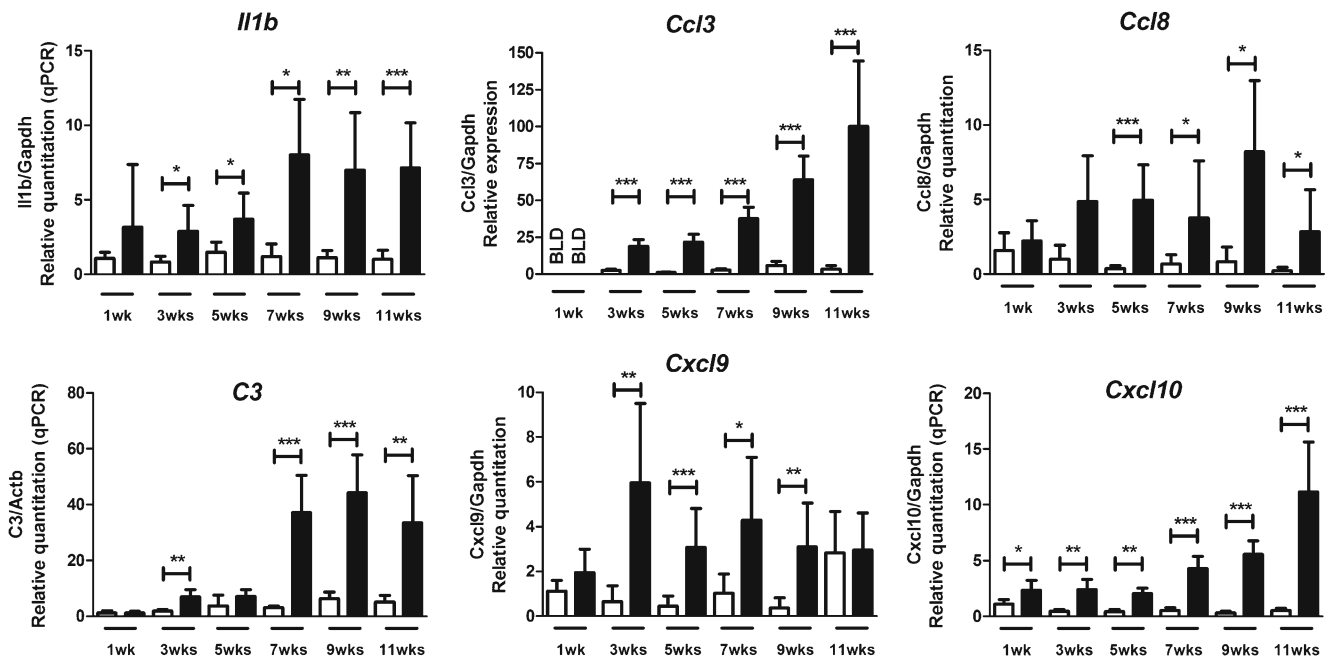
Fig. 1 Validation of mouse inflammation PCR array results. qPCR validation of six genes in $Npc1^{+/+}$ (*white columns*) and $Npc1^{-/-}$ (*black columns*) cerebral cortex. One-week-old control mice were used as reference group for the relative quantitation, except for *Ccl3* for which the 3-week-old control group was used as 1-week-old mice had undetectable transcript levels (BLD: below limit of detection). Mean and standard deviation are shown for each group (N=4). An unpaired t-test with Welch's correction, when necessary, was performed to determine the significance of the difference in means between the log10 values of control and mutant mice relative quantitation at each age: *p-value≤0.05; **p-value≤0.005; ***p-value≤0.0001

progressive dysregulation in the *Npc1* mouse model and increased levels of CCL3 protein in cerebrospinal fluid from NPC1 patients (see below). These data, combined with the prior observation (Wu and Proia 2004) that deletion of the *Ccl3* gene delayed the onset of neurological symptoms and increased survival in a mouse model of GM2-gangliosidosis (Sandhoff disease, *HexB* mutations), prompted us to further characterize the role of *Ccl3* in NPC1 pathology. We hypothesized that, similarly to observations in the *HexB* mutant mouse, deletion of *Ccl3* would improve the phenotype in *Npc1* mutant mice. To test this hypothesis, we intercrossed *Ccl3*-deficient mice with $Npc1^{+/-}$ mice to produce $Npc1^{+/-}Ccl3^{+/-}$ mice. These mice were then intercrossed to obtain $Npc1^{+/+}Ccl3^{+/+}$, $Npc1^{-/-}Ccl3^{+/+}$, $Npc1^{-/-}Ccl3^{+/-}$ and $Npc1^{-/-}Ccl3^{-/-}$ animals on a mixed C57BL/6 and BALB/c background. Most of the $Npc1^{-/-}Ccl3^{+/-}$ and $Npc1^{-/-}Ccl3^{-/-}$ animals showed weight loss and age of death similar to $Npc1^{-/-}Ccl3^{+/+}$ animals, with the notable exception of two double mutant mice that survived to ~13 weeks of age. *Npc1* deficiency in a C57BL/6 genetic background is more severe than in the BALB/c background (Parra et al 2011), thus the mixed genetic background could mask a beneficial effect associated with *Ccl3* deletion. We therefore backcrossed $Npc1^{+/-}Ccl3^{+/-}$ mice to the original BALB/c $Npc1^{+/-}$ animals for five generations (~97 % BALB/c) and compared weight loss and survival of these animals. No significant difference between $Npc1^{-/-}Ccl3^{-/-}$ and $Npc1^{-/-}Ccl3^{+/+}$ mice was

observed (Supplemental Fig. 2). Female $Npc1^{-/-}Ccl3^{+/-}$ and $Npc1^{-/-}Ccl3^{-/-}$ mice gained and maintained a closer-to-normal weight than $Npc1^{-/-}Ccl3^{+/+}$ mice between P40 and P55 days approximately, but all animals with a deletion of the *Npc1* gene had lost 20 % of their maximal weight by approximately 75 days of age. Males with the *Npc1* deletion showed comparable weights at all ages independent of the *Ccl3* genotype.

Expression of genes associated with inflammation in human NPC1 frontal cortex and cerebellar tissue

We tested the presence of neuroinflammation in NPC1 human brains by CD68 immunostaining which is a common microglial activation marker. Frontal cortex and cerebellar tissue from control (Fig. 2a, b) and NPC1 patients (Fig. 2c, d) were analyzed where increased CD68 staining was observed for the NPC1 tissues.

A qPCR array analysis, analogous to that described above for the *Npc1* mouse model, was performed on human frontal cortex and cerebellar brain tissue from control and NPC1 subjects. Nine genes (Table 2a) and ten genes (Table 2b) were differentially expressed with an absolute fold-change ≥2 and p-value≤0.1 for frontal cortex and cerebellar tissue, respectively. Unexpectedly, only one identified gene, complement 3 (*C3*), was concordantly altered in mouse brain, human frontal cortex, and human cerebellar tissue. Interestingly, *CCL5* was
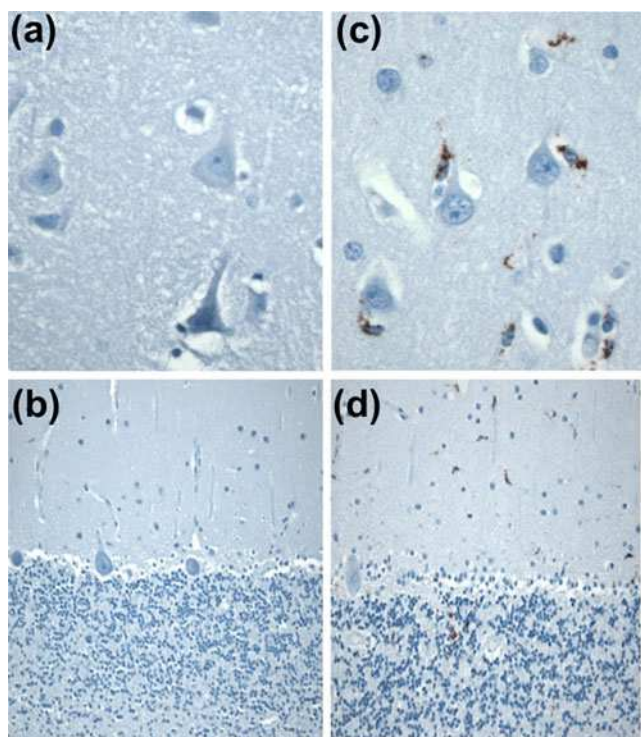
Fig. 2 Representative human tissue stained with the macrophage/microglia marker CD68. The top row shows cortex (400x) from control (**a**) and NPC1 (**c**); The bottom shows cerebellum (200X) from control (**b**) and NPC1 (**d**). Staining was performed on sections from the three patients (UMB#4770, 5372, and M4003M) and respective controls for which brain sections were available. Images are from patient UMB#5372, and control UMB#914

increased in *Npc1* mutant mouse cerebral cortex and in cerebellar tissue from post-mortem NPC1 patients.

qPCR validation was performed for eight of these genes in both frontal cortex and cerebellar tissue from controls and NPC1 patients. We found six genes (*C3*, *CEBP*, *CCR5*, *CXCL5*, *IL10RA*, and *SPP1*) in which significant changes were observed in at least one of the tissue types tested (Supplemental Fig. 3). *C3* expression was higher in NPC1 patients than the age-matched controls, except for the 5-year-old patient (Supplemental Fig. 3a). We additionally evaluated *C4A* (Supplemental Fig. 3b) and *CXCL3* (Supplemental Fig. 3f) gene expression by qPCR, which displayed strong fold-change but not significant p-values on the PCR array data. In general, the expression levels of the ten genes tested were variable within the patient group, which may be related to the degree of variability in disease severity. The 5-year-old male patient showed normal levels of expression of all tested genes in both brain tissue types. The available clinical information indicates that he died

before manifesting neurological symptoms, which might explain why none of these inflammatory-related genes showed altered expression.

Characterization of neuroinflammatory markers in cerebrospinal fluid from NPC1 patients

To expand and translate our findings from the mouse and human arrays, we evaluated neuroinflammatory markers in the cerebrospinal fluid from a cohort of NPC1 patients enrolled in the NIH Natural History/Observational study. This was accomplished by measuring the concentrations of 31 interleukins, cytokines and chemokines in the cerebrospinal fluid of NPC1 patients ($n=42$) and pediatric controls ($n=30$), using multi-analyte ELISA-based profiling (MAP). CSF levels of IL-3 ($p=0.0005$), IL-16 ($p=0.04$), CXCL5 ($p=0.03$) and CCL3 ($p<0.0001$) were increased in NPC1 subjects compared to controls, and CSF levels of IL-4 ($p<0.0001$), IL-10 ($p=0.02$), IL-13 ($p=0.006$) and IL-12p40 ($p<0.0001$) were decreased (Figs. 3 and 4a). Trends were observed for IL-1α ($p=0.06$) and IL-7 ($p=0.07$), while no statistical differences were detected for the interleukins IL-5, IL-6, IL-15 and IL-18 (Supplemental Fig. 4) and MCP-1, MMP3, ICAM-1, or stem cell factor (Supplemental Fig. 5).

The classical pro-inflammatory cytokine TNFα has been shown to be elevated in astrocytes from 7-week-old $Npc1^{-/-}$ mice (Wu et al 2005). Therefore we hypothesized that TNFα would be elevated in the CSF in NPC1 patients as a reflection of the neuroinflammation. Most NPC1 patients had undetectable levels of TNFα in CSF as measured using MAP (limit of detection 1.4 pg/mL). Using a high-sensitivity ELISA kit specific for TNFα, we still found that the majority of tested samples were below the limit of detection (0.1 pg/mL). The TNFα transcript was also measured via the array analysis where no changes were detected in the mouse or human cerebellum but elevation was observed in the human frontal cortex (Table 2a).

Based on the elevated levels of *C3* in both mouse and human tissue samples, we were interested in determining if CSF levels of C3 were altered. As C3 was not evaluated in the MAP experiment, we measured C3 concentrations in CSF from a subset of NPC1 patients and controls from our cohort. No significant differences were observed. Mean CSF C3 levels were 1096±333 ng/mL and 726.6±58.83 ng/mL for control ($n=11$) and NPC1 ($n=14$) samples respectively ($p=0.8$). Another similarity between the array data and CSF data was for *CXCL5*. This gene was found to be elevated in NPC1 patients' tissues (3.9-fold, $p=0.003$ in cerebellum; 4.0-fold, $p=0.03$ in cortex) compared to controls. Furthermore, in the CSF the mean CXCL5 level was found to be mildly elevated in the NPC1 patient cohort (Fig. 3g).

Table 2 **a** Array data displaying altered transcripts in NPC1 human post-mortem frontal cortex tissue versus control tissue. Nine transcripts were altered with a fold-change of ≥2 ($p \leq 0.1$). **b** Transcripts found to be altered in NPC1 post-mortem cerebellar tissue versus control tissue. A total of ten transcripts were altered with a fold-change of ≥2 ($p \leq 0.1$). The two genes listed in the sub-table for each tissue type were found to display drastic fold changes however with p-values > 0.1, but were chosen to validate via qPCR

	Gene symbol	p-value	Fold-change
(A)	Human frontal cortex		
	C3	p<0.005	4.5
	CCL13	0.02	3.4
	CXCL5	0.03	4.0
	IL10RA	0.03	3.8
	IL13RA1	0.02	2.5
	IL17C	0.01	3.9
	IL1R1	0.06	2.7
	LTB	0.07	2.0
	TNF	0.09	5.6
	C4A	0.22	17.3
	CXCL3	0.25	5.1
(B)	Human cerebellum		
	C3	p<0.005	3.3
	CCL5	0.03	5.5
	CCR5	0.08	5.5
	CEBPB	0.01	2.7
	CXCL5	p<0.005	3.9
	IL10RA	0.10	7.9
	IL5	0.05	-2.7
	IL9R	0.05	2.3
	SPP1	0.05	3.5
	TOLLIP	0.05	2.1
	C4A	0.35	3.7
	CXCL3	0.15	3.0

Approximately half of the patients in the NIH Natural History cohort are taking miglustat off-label; therefore, we investigated whether miglustat therapy had any effect on the concentrations of the eight significantly modified markers. IL-3 and IL-13 concentrations were decreased slightly when comparing miglustat treated and untreated patients (p-value <0.05; Supplemental Fig. 6a, e). Since individual responses could be masked by the large degree of inter-patient variation, we compared CSF concentrations of these same eight inflammation markers in five NPC1 patients for whom we had serial cerebrospinal fluid samples prior to and after initiation of off-label miglustat use. In this subset of five patients only IL-10 had a coordinate response (Supplemental Fig. 6d). More extensive, long-term analysis is needed to establish if IL-10 CSF

levels provide a useful indication of neuroinflamation in NPC1 based on these results.

Given the phenotypic heterogeneity observed in NPC1, we were interested in determining if cerebrospinal fluid concentrations of the markers correlated with NPC1 disease status. Using the NIH NPC1 neurological severity score (Yanjanin et al 2010), we observed a significant correlation between CCL3 levels and annual severity increment score (neurological severity score/age; r^2=0.17, p-value<0.002; Fig. 4b).

Discussion

This discovery based analysis revealed several inflammatory markers which are altered in the tissue of *Npc1* mutant mice or NPC1 human tissue specimens relative to controls. The majority of candidate markers from the PCR array in NPC1 post-mortem tissue displayed increased expression in the NPC1 samples relative to controls with only one transcript displaying decreased expression. Inflammation in human NPC1 post-mortem tissue was also confirmed via CD68 staining for activated microglia in both the cerebellum and frontal cortex. Furthermore, measurements of inflammatory markers in cerebrospinal fluid from NPC1 patients and pediatric controls show marked differences for a small set of inflammatory proteins.

Complement C3 was the only gene to be found altered in all samples (mouse cerebral cortex, human cerebellum and human frontal cortex). The expression of some components of the complement pathway had previously been reported as increased in *Npc1* mouse model cerebellum, specifically C1q, C2, C3, C4b and the two receptors C3ar1 and C5r1 (Liao et al 2010; Vazquez et al 2011; Lopez et al 2012a, b). All cell types in the brain are able to produce complement factors (Veerhuis et al 2011), and the complement pathway contributes to the inflammatory process of several brain diseases, including Alzheimer disease (Rubio-Perez and Morillas-Ruiz 2012). A recent study investigating the role of the complement pathway in neuron survival in NPC1 revealed that complement gene deletion did not rescue neuronal death, and therefore innate inflammation, while present in NPC1, is not the major causative factor of neurodegeneration (Lopez et al 2012b).

Activated microglia was observed in brain tissue of the *Npc1* mouse model in several studies via positive CD68 staining (Liu et al 2009; Smith et al 2009; Liao et al 2010; Ramirez et al 2010; Aqul et al 2011; Pressey et al 2012). We also observed this marker of activated microglia in post-mortem tissue from NPC1 patients while it was absent in control tissue. The common classification of "activated microglia" stems from the classical morphological change and the production of neurotoxin or neurotrophic molecules as well as microglia migration to the site of injury.
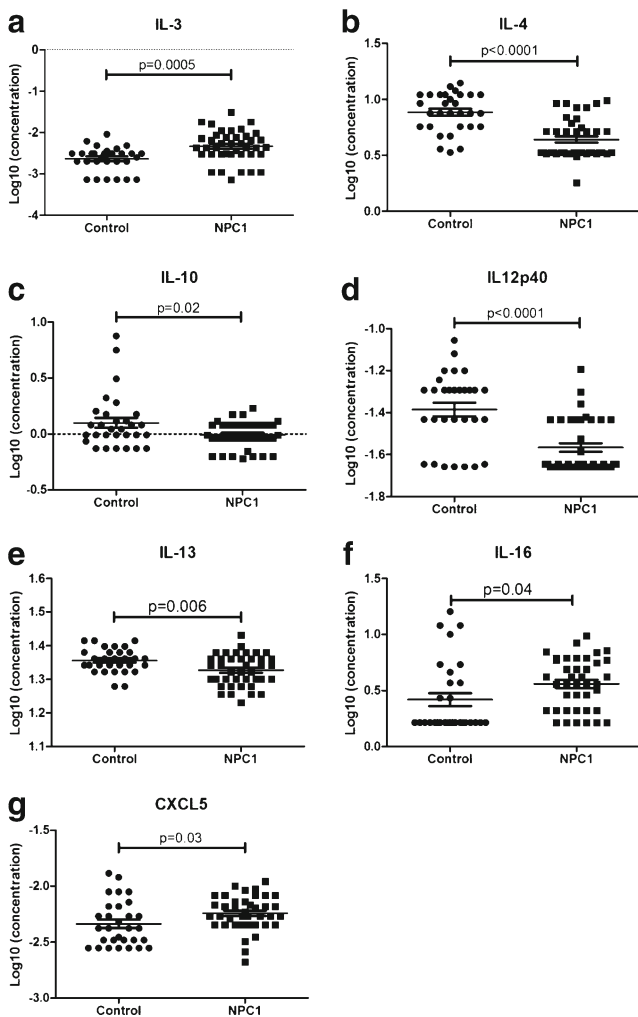
Fig. 3 Cerebrospinal fluid inflammation markers. Log10 transformed concentrations of seven cytokines in cerebrospinal fluid from controls (*circles*) and NPC1 patients (*squares*). Mean and standard deviation are shown for each group. An unpaired *t*-test with Welch's correction when necessary was performed to determine significance

Several classical inflammatory markers have been reported as being dysregulated in the *Npc1* mouse model, including IL1β (Baudry et al 2003; Repa et al 2007) and TNFα (Li et al 2005; Wu et al 2005; Langmade et al 2006; Aqul et al 2011). In our expression study of mouse brain tissue, we identified *Il1b* as being increased. However, it was not modified in human tissues. Similarly, TNFα was only detected as upregulated in NPC1 human cortex tissue. Additionally, both markers were undetectable in cerebrospinal fluid of most NPC1 patients and controls. Other classical markers of inflammation, such as IL-6, IL-8, and MCP1, had comparable levels in patients and controls cerebrospinal fluid, which suggests that the neuroinflammatory mechanism present in NPC1 might be different from a classical neuroinflammation process reported in other disorders.

Eight of the 31 inflammatory markers tested showed significantly different CSF concentrations in NPC1 patients compared to pediatric controls including decreased levels of IL-4 and 10. It has been shown that activated microglia result in the production of IL-4 and IL-10 to reduce neuron degeneration (Park et al 2005; Henry et al 2009); however, the mechanism for IL-10 production within the CNS is still a topic of ongoing research (Chabot et al 1999). Interestingly, little to no change was noted in any of the analyte levels measured from NPC1 patients on miglustat versus those not on miglustat treatments, and only IL-10 displayed a slight decrease after initiation of miglustat therapy. The fact that miglustat treatment did not change the CSF marker levels in NPC1 patients would suggest that the potential anti-inflammatory properties of miglustat may affect classical markers, but not those found to be significantly altered in this study.

From our gene expression experimental results *Ccl3* was found to be altered in the cerebral cortex of 7-week-old *Npc1* mutant mice. In an effort to understand if deletion of this gene would improve the survival and therefore the phenotype of NPC1 disease, we generated a double mutant mouse model. In contrast to the Sandhoff disease model, the genetic deletion of *Ccl3* in the *Npc1* mouse model did not show any improvement with regards to survival or weight loss in the *Npc1* mutant animals. This suggests that the origins of the brain inflammation observed in the two lysosomal storage diseases are likely different. In particular, macrophage infiltration from the periphery is observed in Sandhoff disease (Wu and Proia 2004), and does not appear to occur in NPC1 disease (Lopez et al 2012a). The effect of *Ccl3* deletion in *Npc1* mice has been reported in the F1 generation (Lopez et al 2012a). In agreement with our finding, the authors did not observe an improvement in the double *Npc1* and *Ccl3* mutant phenotype compared to the *Npc1* mutants. However, they reported a lower weight in double-mutant males compared to $Npc1^{-/-}$ $Ccl3^{+/+}$, and a slightly shorter survival rate, but no differences between females. On the contrary, we observed a small temporary benefit in weight gain for $Npc1^{-/-}$ females with deletion of one or two *Ccl3* alleles, and no differences for males. Genetic background might have an impact on this specific trait, as $Npc1^{-/-}$ mice have a more severe phenotype on a C57BL/6 background than on a BALB/c background (Parra et al 2011). Considering that we backcrossed our mice for five generations, the effect of the C57BL/6 background was probably negligible in our cohort of animals.

Despite the absence of a positive effect of *Ccl3* deletion on NPC1 disease process, we identified increased concentrations of CCL3 in cerebrospinal fluid of NPC1 patients compared to age-matched controls. Correlation of CCL3 levels with disease severity and the clear separation of the patient group compared to controls make CCL3 an
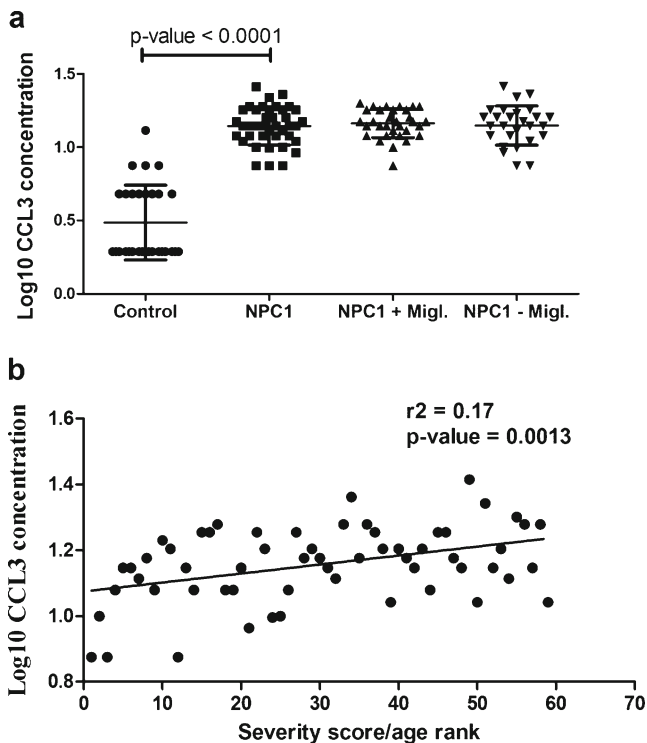
Fig. 4 CCL3 marker. **a** Log10 transformed concentrations of CCL3 in cerebrospinal fluid from controls (*circles*) and NPC1 patients (*squares*). The patient group was additionally separated between patients receiving miglustat treatment (*triangles*), and patients not receiving miglustat treatment (*inverted triangles*). Mean and standard deviation are shown for each group. An unpaired *t*-test with Welch's correction when necessary was performed to determine the significance of the difference in means between controls and patients. **b** Correlation of CCL3 concentrations in cerebrospinal fluid with patient annual severity increment score (severity score divided by their age) followed by numerical ranking (i.e., 1 to 59 representing least to most severe phenotype)

interesting biomarker for evaluation of NPC1 disease status. Future studies aimed at developing an appropriate pharmacological therapy for NPC1 disease will be strengthened by the ability to monitor CCL3 CSF concentration in these patients.

To summarize, extensive work conducted within the last decade has documented a progressive inflammatory process occurring in NPC1 disease. The vast majority of this work has focused on the *Npc1* mouse model. We therefore investigated the neuroinflammatory process in NPC1 patients. Based on our studies, we have identified several potential inflammatory markers that may prove useful in correlating with neurological progression or be utilized to facilitate the design and implementation of clinical trials to demonstrate potential efficacy of candidate therapies.

References

Aqul A, Liu B, Ramirez CM et al (2011) Unesterified cholesterol accumulation in late endosomes/lysosomes causes neurodegeneration and is prevented by driving cholesterol export from this compartment. J Neurosci 31(25):9404–9413

Baudry M, Yao Y, Simmons D, Liu J, Bi X (2003) Postnatal development of inflammation in a murine model of Niemann-Pick type C disease: immunohistochemical observations of microglia and astroglia. Exp Neurol 184(2):887–903

Carstea ED, Morris JA, Coleman KG et al (1997) Niemann-Pick C1 disease gene: homology to mediators of cholesterol homeostasis. Science 277(5323):228–231

Chabot S, Williams G, Hamilton M, Sutherland G, Yong VW (1999) Mechanisms of IL-10 production in human microglia-T cell interaction. J Immunol 162(11):6819–6828

Davidson CD, Ali NF, Micsenyi MC et al (2009) Chronic cyclodextrin treatment of murine Niemann-Pick C disease ameliorates neuronal cholesterol and glycosphingolipid storage and disease progression. PLoS One 4(9):e6951

Eng LF, Ghirnikar RS, Lee YL (2000) Glial fibrillary acidic protein: GFAP-thirty-one years (1969–2000). Neurochem Res 25(9–10):1439–1451

Fu R, Yanjanin NM, Bianconi S, Pavan WJ, Porter FD (2010) Oxidative stress in Niemann-Pick disease, type C. Mol Genet Metab 101(2–3):214–218

Ganser GH, Hewett P (2010) An accurate substitution method for analyzing censored data. J Occup Environ Hyg 7(4):233–244

Graeber MB, Li W, Rodriguez ML (2011) Role of microglia in CNS inflammation. FEBS Lett 585(23):3798–3805

Henry CJ, Huang Y, Wynne AM, Godbout JP (2009) Peripheral lipopolysaccharide (LPS) challenge promotes microglial hyperactivity in aged mice that is associated with exaggerated induction of both pro-inflammatory IL-1beta and anti-inflammatory IL-10 cytokines. Brain Behav Immun 23(3):309–317

Klein A, Maldonado C, Vargas LM et al (2011) Oxidative stress activates the c-Abl/p73 proapoptotic pathway in Niemann-Pick type C neurons. Neurobiol Dis 41(1):209–218

Kunisch E, Fuhrmann R, Roth A, Winter R, Lungershausen W, Kinne RW (2004) Macrophage specificity of three anti-CD68 monoclonal antibodies (KP1, EBM11, and PGM1) widely used for immunohistochemistry and flow cytometry. Ann Rheum Dis 63(7):774–784

Langmade SJ, Gale SE, Frolov A et al (2006) Pregnane X receptor (PXR) activation: a mechanism for neuroprotection in a mouse model of Niemann-Pick C disease. Proc Natl Acad Sci USA 103(37):13807–13812

Li H, Repa JJ, Valasek MA et al (2005) Molecular, anatomical, and biochemical events associated with neurodegeneration in mice with Niemann-Pick type C disease. J Neuropathol Exp Neurol 64(4):323–333

Liao G, Wen Z, Irizarry K et al (2010) Abnormal gene expression in cerebellum of Npc1−/− mice during postnatal development. Brain Res 1325:128–140

Liu B, Ramirez CM, Miller AM, Repa JJ, Turley SD, Dietschy JM (2010) Cyclodextrin overcomes the transport defect in nearly every organ of NPC1 mice leading to excretion of sequestered cholesterol as bile acid. J Lipid Res 51(5):933–944

Liu B, Turley SD, Burns DK, Miller AM, Repa JJ, Dietschy JM (2009) Reversal of defective lysosomal transport in NPC disease ameliorates liver dysfunction and neurodegeneration in the npc1−/− mouse. Proc Natl Acad Sci USA 106(7):2377–2382

Livak KJ, Schmittgen TD (2001) Analysis of relative gene expression data using real-time quantitative PCR and the 2(−Delta Delta C(T)) Method. Methods 25(4):402–408

Loftus SK, Morris JA, Carstea ED et al (1997) Murine model of Niemann-Pick C disease: mutation in a cholesterol homeostasis gene. Science 277(5323):232–235

Lopez ME, Klein AD, Hong J, Dimbil UJ, Scott MP (2012a) Neuronal and epithelial cell rescue resolves chronic systemic inflammation in the lipid storage disorder Niemann-Pick C. Hum Mol Genet 21(13):2946–2960

Lopez ME, Klein AD, Scott MP (2012b) Complement is dispensable for neurodegeneration in Niemann-Pick disease type C. J Neuroinflamm 9(1):216

Love S, Bridges LR, Case CP (1995) Neurofibrillary tangles in Niemann-Pick disease type C. Brain 118(Pt 1):119–129

Marin-Teva JL, Cuadros MA, Martin-Oliva D, Navascues J (2012) Microglia and neuronal cell death. Neuron Glia Biol 7(1):25-40.

Ong WY, Kumar U, Switzer RC et al (2001) Neurodegeneration in Niemann-Pick type C disease mice. Exp Brain Res 141(2):218–231

Park KW, Lee DY, Joe EH, Kim SU, Jin BK (2005) Neuroprotective role of microglia expressing interleukin-4. J Neurosci Res 81(3):397–402

Parra J, Klein AD, Castro J et al (2011) Npc1 deficiency in the C57BL/6J genetic background enhances Niemann-Pick disease type C spleen pathology. Biochem Biophys Res Commun 413(3):400–406

Patterson MC, Vecchio D, Jacklin E et al (2010) Long-term miglustat therapy in children with Niemann-Pick disease type C. J Child Neurol 25(3):300–305

Patterson MC, Vecchio D, Prady H, Abel L, Wraith JE (2007) Miglustat for treatment of Niemann-Pick C disease: a randomised controlled study. Lancet Neurol 6(9):765–772

Pentchev PG, Comly ME, Kruth HS et al (1987) Group C Niemann-Pick disease: faulty regulation of low-density lipoprotein uptake and cholesterol storage in cultured fibroblasts. FASEB J 1(1):40–45

Pineda M, Wraith JE, Mengel E et al (2009) Miglustat in patients with Niemann-Pick disease Type C (NP-C): a multicenter observational retrospective cohort study. Mol Genet Metab 98(3):243–249

Porter FD, Scherrer DE, Lanier MH et al (2010) Cholesterol oxidation products are sensitive and specific blood-based biomarkers for Niemann-Pick C1 disease. Sci Trans Med 2(56):56ra81

Pressey SN, Smith DA, Wong AM, Platt FM, Cooper JD (2012) Early glial activation, synaptic changes and axonal pathology in the thalamocortical system of Niemann-Pick type C1 mice. Neurobiol Dis 45(3):1086–1100

Ramirez CM, Liu B, Taylor AM et al (2010) Weekly cyclodextrin administration normalizes cholesterol metabolism in nearly every organ of the Niemann-Pick type C1 mouse and markedly prolongs life. Pediatr Res 68(4):309–315

Ransohoff RM, Brown MA (2012) Innate immunity in the central nervous system. J Clin Invest 122(4):1164–1171

Reddy JV, Ganley IG, Pfeffer SR (2006) Clues to neuro-degeneration in Niemann-Pick type C disease from global gene expression profiling. PLoS One 1:e19

Repa JJ, Li H, Frank-Cannon TC et al (2007) Liver X receptor activation enhances cholesterol loss from the brain, decreases neuroinflammation, and increases survival of the NPC1 mouse. J Neurosci 27(52):14470–14480

Rubio-Perez JM, Morillas-Ruiz JM (2012) A review: inflammatory process in Alzheimer's disease, role of cytokines. SciWorld J 2012:756357

Sarna JR, Larouche M, Marzban H, Sillitoe RV, Rancourt DE, Hawkes R (2003) Patterned Purkinje cell degeneration in mouse models of Niemann-Pick type C disease. J Comp Neurol 456(3):279–291

Smith D, Wallom KL, Williams IM, Jeyakumar M, Platt FM (2009) Beneficial effects of anti-inflammatory therapy in a mouse model of Niemann-Pick disease type C1. Neurobiol Dis 36(2):242–251

Stein VM, Crooks A, Ding W et al (2012) Miglustat improves purkinje cell survival and alters microglial phenotype in feline Niemann-Pick disease type C. J Neuropathol Exp Neurol 71(5):434–448

Suk K (2010) Combined analysis of the glia secretome and the CSF proteome: neuroinflammation and novel biomarkers. Expert Rev proteomics 7(2):263–274

Suzuki K, Parker CC, Pentchev PG et al (1995) Neurofibrillary tangles in Niemann-Pick disease type C. Acta Neuropathol 89(3):227–238

Vanier MT (2010) Niemann-Pick disease type C. Orphanet J Rare Dis 5:16

Vanier MT, Millat G (2003) Niemann-Pick disease type C. Clin Genet 64(4):269–281

Vazquez MC, Del Pozo T, Robledo FA et al (2011) Alteration of gene expression profile in niemann-pick type C mice correlates with tissue damage and oxidative stress. PLoS One 6(12):e28777

Veerhuis R, Nielsen HM, Tenner AJ (2011) Complement in the brain. Mol Immunol 48(14):1592–1603

Ward S, O'Donnell P, Fernandez S, Vite CH (2010) 2-hydroxypropyl-beta-cyclodextrin raises hearing threshold in normal cats and in cats with Niemann-Pick type C disease. Pediatr Res 68(1):52–56

Wraith JE, Vecchio D, Jacklin E et al (2010) Miglustat in adult and juvenile patients with Niemann-Pick disease type C: long-term data from a clinical trial. Mol Genet Metab 99(4):351–357

Wu YP, Mizukami H, Matsuda J, Saito Y, Proia RL, Suzuki K (2005) Apoptosis accompanied by up-regulation of TNF-alpha death pathway genes in the brain of Niemann-Pick type C disease. Mol Genet Metab 84(1):9–17

Wu YP, Proia RL (2004) Deletion of macrophage-inflammatory protein 1 alpha retards neurodegeneration in Sandhoff disease mice. Proc Natl Acad Sci USA 101(22):8425–8430

Yanjanin NM, Velez JI, Gropman A et al (2010) Linear clinical progression, independent of age of onset, in Niemann-Pick disease, type C. Am J Med Genet B Neuropsychiatr Genet 153B(1):132–140

Zampieri S, Mellon SH, Butters TD et al (2009) Oxidative stress in NPC1 deficient cells: protective effect of allopregnanolone. J Cell Mol Med 13(9B):3786–3796

Zervas M, Dobrenis K, Walkley SU (2001) Neurons in Niemann-Pick disease type C accumulate gangliosides as well as unesterified cholesterol and undergo dendritic and axonal alterations. J Neuropathol Exp Neurol 60(1):49–64